# Supplemental Materials

***Molecular Biology of the Cell***

Raya-Sandino *et al*.

## Supplemental figure 1

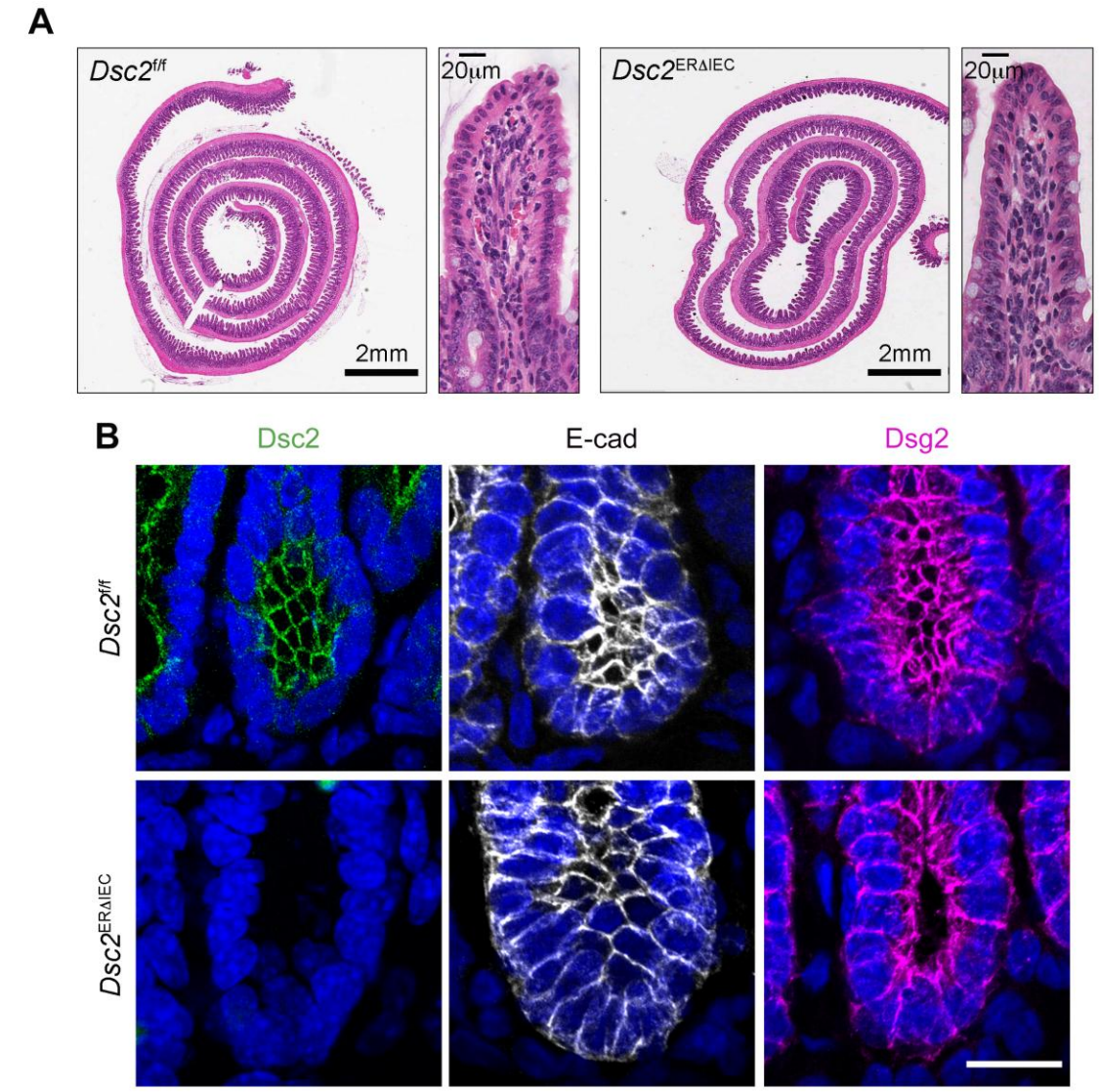

**Supplemental figure 1.** (A) Gross architecture of the ileum is not affected by the depletion of Dsc2 on IECs *in vivo*. Paraffin-embedded sections of terminal ileal tissue from *Dsc2*$^{f/f}$ and *Dsc2*$^{ER\Delta IEC}$ mice were stained with Hematoxylin and Eosin for histological examination. Overall mucosal architecture is intact and, crypt and villus length was unaltered. Scale bars: 2mm overview, 20µm inserts. (B) Representative images of colon tissue sections from tamoxifen-treated *Dsc2*$^{ER\Delta IEC}$ and *Dsc2*$^{f/f}$ mice stained with anti-Dsc2, anti-Dsg2 or anti-E-cadherin antibodies and DAPI as a nuclear counterstain. Dsc2 expression is absent in *Dsc2*$^{ER\Delta IEC}$ mice with no change in Dsg2 and E-cadherin expression. Scale bar is 25µm.

**Supplemental figure 2**

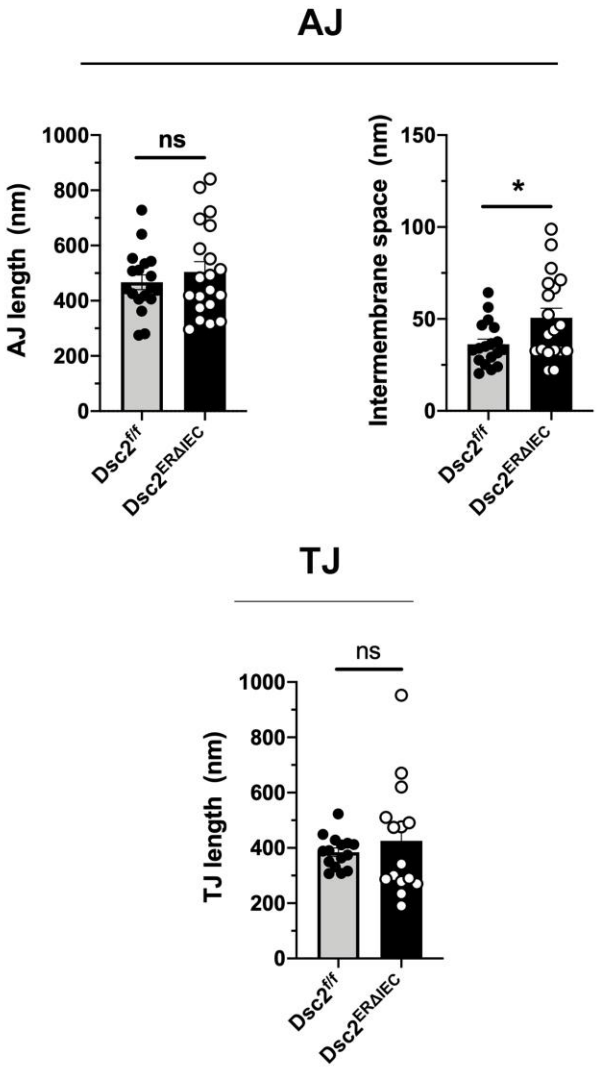

**Supplemental figure 2.** Dsc2 deficiency on IECs increases AJ intermembrane space. Histograms represent length of AJ and TJ as well as intermembrane space (IMS) of AJ measured from transmission electron microscopy images of the intercellular junctions between adjacent IECs in the ileum of *Dsc2*$^{ER\Delta IEC}$ and *Dsc2*$^{fl/fl}$ mice. Histograms show the mean ± SEM. Points represent values from individual AJ and TJ for a total of 3 mice per group. 18 AJs were analyzed for *Dsc2*$^{fl/fl}$ mice and 20 AJs for *Dsc2*$^{ER\Delta IEC}$. 15 TJs were analyzed for *Dsc2*$^{fl/fl}$ and *Dsc2*$^{ER\Delta IEC}$ mice. Statistical analysis was done with two-tailed Student's *t* test. ns, not significant; *$p < 0.05$.

**Supplemental figure 3**

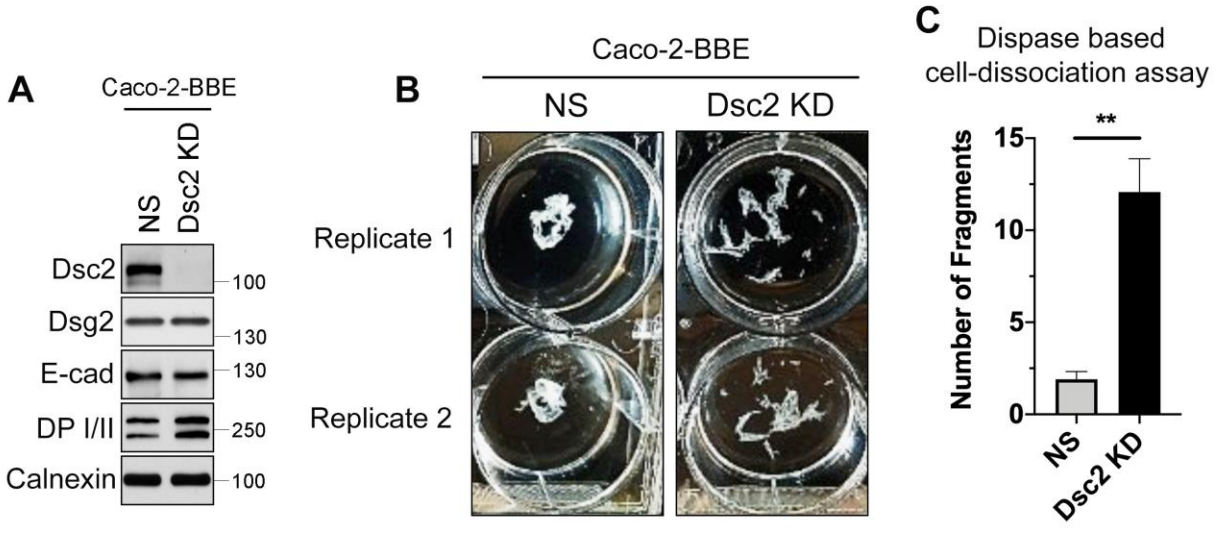

**Supplemental figure 3.** Loss of Dsc2 in Caco-2-BBE decreases intercellular adhesion. (A) shRNA-induced knockdown of Dsc2 in human IEC line, Caco-2-BBE was confirmed by Western blotting. The expression of Dsg2 and E-cadherin were unchanged although DP I/II was augmented. (B) Confluent monolayers of Dsc2 knockdown or control cells were subjected to a dispase II-based cell dissociation assay and the number of fragments were quantified. (C) Loss of Dsc2 resulted in increased number of fragments in comparison to control cells supporting decreased intercellular adhesion. Results show the mean ± SEM of data combined from three individual experiments, each one assayed in two technical replicates. Statistical analysis was done with two-tailed Student's *t* test. **$p < 0.01$.

**Supplemental figure 4**

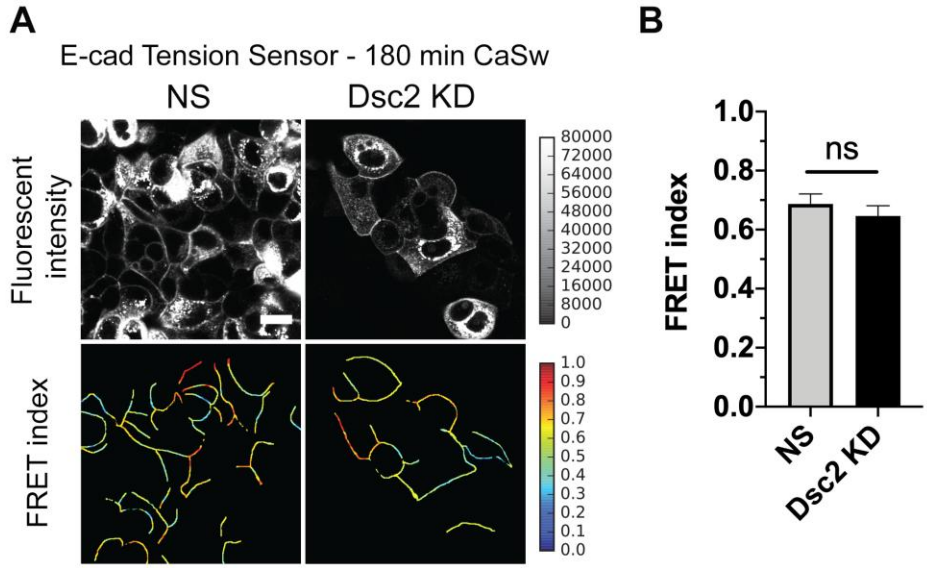

**Supplemental figure 4.** Depletion of Dsc2 did not affect E-cadherin tension force after calcium switch. SKCO-15 Dsc2 KD or control cells were transduced with vector expressing an E-cadherin tension sensor (E-cad TS). Monolayers expressing an E-cad TS showed no significant difference in tension force on AJ (depicted by the FRET index measurements) between SKCO-15 non-silencing (NS) and Dsc2 KD cells, during cell-cell junction recovery after 180 min of calcium repletion. (A) Representative color-coded images of three independent experiments, where cold and hot colors respectively indicate low and high levels of FRET index on E-cadherin, respectively**.** Scale bar is 20μm. (B) Histogram represents the average FRET index. Statistical analysis was done with two-tailed Student's *t* test. ns, not significant.

**Supplemental figure 5**

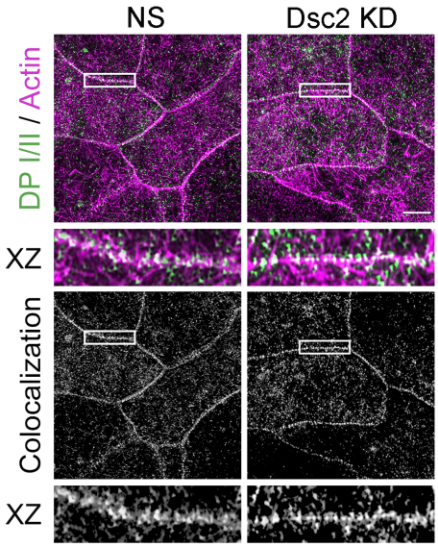

**Supplemental figure 5.** The association of DP I/II with the actin cytoskeleton is not perturbed by loss of Dsc2. Structured illumination microscopy images showing DP I/II (green) and F-actin (magenta) in SKCO-15 control (NS) and Dsc2 KD cells. Rectangles mark zoomed in areas. Scale bar is 5μm.